Inorg. Chem. **2005**, *44*, 251–257

New Titanium and Nickel Gallophosphates with Layered Structures

Chia-Her Lin and Sue-Lein Wang*

Department of Chemistry, National Tsing Hua University, Hsinchu 300, Taiwan

Received April 28, 2004

Two new transition-metal gallophosphates, $(H_2C_4H_{10}N_2)_3[(Ti_{2.5}(H_2O)_4Ga_{5.5}(PO_4)_{10}]\cdot 2H_2O$ (**TGP-1**) and $[H_{3.5}(C_4H_{13}N_3)_2]$-$[(Ni_{0.5}(OH)_4Ga_{5.5}(PO_4)_3(HPO_4)_4]\cdot 2H_2O$ (**NGP-1**), have been synthesized under mild hydrothermal conditions and characterized by single-crystal X-ray diffraction, thermogravimetric analysis, electron paramagnetic resonance, electron probe microanalysis, and magnetic susceptibility data. **TGP-1** exhibits a unique two-dimensional structure consisting of tetrahedral and octahedral metals centers and is the foremost paramagnetic TiGaPO material ever prepared. **NGP-1** as well represents the first NiGaPO compound and adopts a layer structure that is constructed from hexameric M–O clusters of trigonal bipyramids and octahedra. In both compounds, the transition metals incorporate with gallium into octahedral sites only, while the four- and five-coordinated metals centers are only Ga^{3+} ions. The unique sites for Ti^{3+} and Ni^{2+} ions have been initially elucidated from single-crystal structure refinements and further confirmed by bond-valence-sum calculations, EPR, and magnetic susceptibility studies. Crystal data: **TGP-1**, monoclinic, $P2_1/c$, $a = 25.692(2)$ Å, $b = 9.6552(8)$ Å, $c = 9.8418(8)$ Å, $\beta = 96.737(2)°$, $V = 2424.5(3)$ Å^3, and $Z = 2$; **NGP-1**, monoclinic, $C2/c$, $a = 20.8363(12)$ Å, $b = 11.9546(7)$ Å, $c = 16.4577(9)$ Å, $\beta = 117.285(1)°$, $V = 3643.3(1)$ Å^3, $Z = 4$.

Introduction

Research development in microporous inorganic materials has flourished in the past decade due to diversity of structures, interesting properties, and potential applications in sorption, ion exchange, heterogeneous catalysis, and microelectronics.[1−5] Incorporation of transition-metal (TM) ions into microporous solids, such as silicates, aluminosilicates, alumino- and gallophosphates, has been proven to be a favorable approach for preparing catalytically enhanced molecular sieves[4−7] or for creating new microporous solids.[6−10] In the former cases, the nature of active sites is of considerable importance in understanding the catalytic behavior and designing novel catalysts. In principle, the exact location and immediate environments of TM sites can be directly obtained from structure analysis. However, it has not been so straightforward due to lack of suitable crystals.[5,11] Titanium, for example, is of great interest for its high ability in improving catalytic selectivity,[12] yet no real evidence can be given for a substitution of phosphorus or gallium sites by titanium in Ti−CLO.[13] Besides isomorphous substitution, on the other hand, TM ions can often lead to the formation of new framework topologies. For example, by implanting vanadium, manganese, cobalt, copper, and zinc into GaPO lattices, novel structures had been generated.[7,8,14−22] However,

* To whom correspondence should be addressed. E-mail: slwang@mx.nthu.edu.tw.

(1) Davis, M. E. *Nature* **2002**, *417*, 813.
(2) Cheetham, A. K.; Férey, G.; Loiseau, T. *Angew. Chem., Int. Ed.* **1999**, *38*, 3268.
(3) Corma, A. *Chem. Rev.* **1995**, *9*, 5, 559.
(4) Thomas, J. M. *Angew. Chem., Int. Ed.* **1999**, *38*, 3588.
(5) Hartmann, M.; Kevan, L. *Chem. Rev.* **1999**, *635*, 5.
(6) Bu, X.; Feng, P.; Stucky, G. D. *Nature* **1997**, *388*, 735.
(7) Bu, X.; Feng, P.; Stucky, G. D. *Science* **1997**, *278*, 2080.
(8) Chippindale, A. M.; Cowley, A. R. *Microporous Mesoporous Mater.* **1998**, *21*, 271
(9) Noble, G. W.; Wright, P. A.; Lightfoot, P.; Morris, R. E.; Hudson, K. J.; Kvick, ˚A.; Graafsma, H. *Angew. Chem., Int. Ed. Engl.* **1997**, *36*, 81.
(10) Beitone, L.; Huguenard, C.; Gansmuller, A.; Henry, M.; Taulelle, F.; Loiseau, T.; Férey, G. *J. Am. Chem. Soc.* **2003**, *125*, 9102.
(11) Zahedi-Niaki, M.; Joshi, P.; Kaliaguine, S. *Chem. Commun.* **1996**, 47.
(12) (a) Anderson, M. W.; Tarasaki, O.; Oshuna, T.; Philippou, A.; Mackay, S. P.; Ferreira, A.; Rocha, J.; Lidin, S. *Nature* **1994**, *367*, 347. (b) Bianchi, C.; Ragaini, V. *J. Catal.* **1997**, *168*, 70. (c) Rocha, J.; Anderson, M. W. *Eur. J. Inorg. Chem.* **2000**, 801.
(13) Zubowa, H.; Schreier, E.; Jancke, K.; Steinike, U. *Collect. Czech. Chem. Commun.* **1995**, *60*, 403.
(14) Lin, C. H.; Wang, S. L. *Chem. Mater.* **2002**, *14*, 96.
(15) Lin, C. H.; Wang, S. L. *Chem. Mater.* **2000**, *12*, 3617.
(16) Hsu, K. F.; Wang, S. L. *Chem. Commun.* **2000**, 135.
(17) Hsu, K. F.; Wang, S. L. *Inorg. Chem.* **2000**, *39*, 1773.
(18) A new series of VGaPOs has been prepared: Huang, L. H.; Wang, S. L, to be submitted.
(19) Chippindale, A. M.; Cowley, A. R. *J. Solid State Chem.* **2001**, *159*, 59.
(20) Chippindale, A. M.; Bond, A. D.; Cowley, A. R., Powell, A. V. *Chem. Mater.* **1997**, *9*, 2830.
(21) Wragg, D.; Morris, R. E. *J. Mater. Chem.* **2001**, *11*, 513−517.
(22) Logar, N. Z.; Mrak, M.; Kaučič, V. *J. Solid State Chem.* **2001**, *156*, 480.

10.1021/ic0494556 CCC: $30.25
Published on Web 12/29/2004

no report on Ti-, Cr-, and Ni-incorporated GaPOs have ever been documented. In our recent investigations on zeolitic organo-metallophosphates,[23] we have not only incorporated Cr^{3+} ions into the 24R-channel NTHU-1[24] but also successfully prepared a unique TiGaPO, $(H_2C_4H_{10}N_2)_3[(Ti_{2.5}(H_2O)_4Ga_{5.5}(PO_4)_{10}]\cdot 2H_2O$ (designated **TGP-1**), and a new NiGaPO, $[H_{3.5}(C_4H_{13}N_3)_2][(Ni_{0.5}(OH)_4Ga_{5.5}(PO_4)_3(HPO_4)_4]\cdot 2H_2O$ (designated **NGP-1**). Herein, we report the hydrothermal syntheses, thermal analysis, crystal structures, characterization on the titanium(III) and nickel(II) sites, magnetic susceptibility, and EPR data of the first members in the TiGaPO and NiGaPO systems.

Experimental Section

Synthesis and Compositional Characterization. Chemicals of reagent grade or better were used as received and all reactions were carried out in Teflon-lined digestion bombs (internal volume of 23 mL) under autogenous pressure by heating the reaction mixtures at 160 °C for 3 days followed by slow cooling at 6 °C h^{-1} to room temperature. Lamellate crystals of **TGP-1** were initially obtained from a reaction mixture of piperazine ($C_4H_{10}N_2$, PIP, 3 mmol), Ga_2O_3 (0.75 mmol), titanium powder (325 mesh, 1.5 mmol), H_3PO_4(aq) (85%, 9.0 mmol), and H_2O (12.0 mL). The product was a multiphase and comixed by unreacted Ti powders. An optimum condition for preparing a nearly single-phased product can be achieved by changing the molar ratios of $PIP/Ga_2O_3/Ti/H_3PO_4$ to 3.45:0.50:1.0:6.0. The final product consisted of unavoidable minimum residual Ti powders and crystallites of **TGP-1**, whose color is similar to rose quartz and indicates the presence of Ti^{3+} ions. To incorporate divalent Ni atoms, the template was switched to a triamine, diethylenetriamine (DETA). Under the same reaction conditions with $NiCl_2$ replacing Ti and the triamine DETA replacing the diamine PIP, a product containing greenish crystals of **NGP-**1 as a major phase were obtained. Powder XRD measurements were performed on picked crystals to confirm the phase purity before all chemical and physical analyses. Elemental analyses were carried out to confirm the organic contents. Anal. found/calcd: C, 7.61/7.90; N, 4.43/4.61; H, 2.73/2.65 for **TGP-1**; C, 6.54/6.88; N, 5.43/6.02; H, 2.97/2.96 for **NGP-1**. For **TGP-1**, the M to Ga ratios determined from single-crystal structure analyses (vide infra) were further confirmed by electron probe microanalysis (EPMA) data.

Single-Crystal Structure Analysis. Crystals of dimensions 0.25 × 0.25 × 0.05 mm for **TGP-1** and 0.40 × 0.40 × 0.10 mm for **NGP-1** were selected for indexing and intensity data collection. The diffraction measurements were performed on Bruker-AXS Smart-CCD diffractometers ($\lambda = 0.71073$ Å). Intensity data were collected in 1271 frames with increasing ω (0.3° per frame) and corrected for Lp and absorption effects using the SADABS program.[25] Number of measured/unique reflections with $I > 2\sigma_I$: 14110/5495 for **TGP-1** and 9395/3871 for **NGP-1**. On the basis of systematic absences and statistics of intensity distribution, the space groups were determined to be $P2_1/c$ for **TGP-1** and $C2/c$ for **NGP-1**. Both structures were solved by direct methods with Ga and P atoms disclosed first, followed by the atoms O, N, and C located on successive difference Fourier maps. The location of Ti in **TGP-1** or Ni in **NGP-1** was initially speculated from abnormal thermal parameters and partial occupancy of the octahedral Ga centers. Subsequent structure refinements on occupancies with the sums constraint to 1.00 for each individual metal site were carried out and the results indicated that all octahedral sites were partially substituted by TM atoms. For **TGP-1**, the site of M(3) is occupied by 50% Ti and 50% Ga and that of M(4) is 75% Ti and 25% Ga, and for **NGP-1**, the site of M(2) is 15% Ni and 85% Ga and that of M(3) is 10% Ni and 90% Ga. The ratios of Ti/Ga/P determined from single-crystal structure refinements (2.5:5.5:10) can be compared well with EPMA data (2.4:5.1:10.0) measured from that particular crystal. Water oxygens O(21) and O(22) in **TGP-1** and the hydroxo oxygen atoms O(15) and O(16) and the water oxygen O(17) in **NGP-1** were all identified from their unsaturated bond-valence sums.[26] The last cycles of refinement, based on F^2, including atomic positions for all atoms, anisotropic thermal parameters for all non-hydrogen framework atoms, and isotropic thermal parameters for all the hydrogen atoms, converged at R1 = 0.0399 for **TGP-1** and R1 = 0.0424 for **NGP-1**. Corrections for secondary extinction and anomalous dispersion were applied. Neutral-atom scattering factors for all atoms were taken from the standard sources. All calculations were performed by using SHELXTL programs.[25] Crystallographic data are given in Table 1. Atomic coordinates (except the organic part) and thermal parameters are in Tables 2 and 3, and selected bond distances are in Tables 4 and 5. Other details for the refinements are given in the Supporting Information.

Table 1. Crystallographic Data for **TGP-1** and **NGP-1**

	TGP-1	**NGP-1**
formula	$C_{12}H_{48}Ga_{5.5}N_6O_{46}P_{10}Ti_{2.5}$	$C_8H_{41}Ga_{5.5}N_6Ni_{0.5}O_{34}P_7$
fw	1825.40	1395.07
space group	$P2_1/c$	$C2/c$
a, Å	25.692(2)	20.8363(12)
b, Å	9.6552(8)	11.9546(7)
c, Å	9.8418(8)	16.4577(9)
β, deg	96.737(2)	117.285(1)
volume, Å^3	2424.5(3)	3643.3(4)
Z	2	4
D_{calc}, g cm^{-3}	2.416	2.524
μ, mm^{-1}	3.795	4.587
T, °C	22	22
λ, Å	0.71073	0.71073
R1[a]	0.0399	0.0424
wR2[b]	0.1048	0.1253

[a] $R1 = \sum||F_o| - |F_c||/\sum|F_o|$ for $F_o > 4\sigma(F_o)$. [b] $wR2 = [\sum[w(|F_o|^2 - |F_c|^2)^2]/\sum w(|F_o|^2)^2]^{1/2}$ for all data, where $w = [2(F_o^2) + 0.0666P]^2 + 1.01P$ for **TGP-1** and $w = [2(F_o^2) + 0.0737P]^2 + 48.21P$ for **NGP-1**.

Thermal Study. Thermalgravimetric analyses (TGA), using a Seiko TG 300 analyzer, were performed on powder samples of **TGP-1** and **NGP-1** under flowing N_2 with a heating rate of 10 °C/min. The TG curves are shown in Figure 1. For **TGP-1**, the curve involves a partially resolved two-step weight loss before 300 °C: from 50 to ca. 120 °C for the dehydration of two lattice water (calcd 2.0%) and ca. 120−300 °C for release of four coordination water molecules (calcd 3.9%). Further weight loss, from ca. 300 to 1100 °C, should be attributed to the decomposition of organic cations (calcd 14.2% for 3PIP and 3.0% for $3H_2O$). For **NGP-1**, the weight loss that occurred before ca. 150 °C should correspond to two lattice water molecules (calcd 2.6%), while that between 150 and 350 °C corresponds to the release of solvate DETA molecule (calcd 7.4%), and that beyond ca. 350 °C is attributed to the decomposition of organic cations. For both compounds, the structures become amorphous after templates were removed, and further heating to 1100 °C resulted in $GaPO_4$ (JCPDF no. 16-0185) as a major phase in the final residuals.

(23) Liao, Y. C.; Liao, F. L.; Chang, W. K.; Wang, S. L. *J. Am. Chem. Soc.* **2004**, *126*, 1320.
(24) Lin, C. H.; Wang, S. L.; Lii, K. H. *J. Am. Chem. Soc.* **2001**, *123*, 4649.
(25) Bruker Analytical X-ray Systems, *SHELXTL programs*, Release Version 5.1, **1998**.
(26) Brown, I. D.; Altermann, D. *Acta Crystallogr.* **1985**, *B41*, 244.

Table 2. Atomic Coordinates ($\times 10^4$) and Thermal Parameters (Å^2 $\times$ 10^3) for **TGP-1**

	x	*y*	*z*	*U*(eq)[a]
Ga(1)	3684(1)	6418(1)	4840(1)	11(1)
Ga(2)	1646(1)	3712(1)	3407(1)	13(1)
M(3)[b]	4746(1)	1321(1)	7758(1)	10(1)
M(4)[c]	1708(1)	7205(1)	986(1)	11(1)
P(1)	1879(1)	3860(1)	367(1)	11(1)
P(2)	4390(1)	3937(1)	5869(1)	11(1)
P(3)	933(1)	8781(1)	−1664(1)	13(1)
P(4)	2440(1)	6092(1)	3948(1)	11(1)
P(5)	4171(1)	8358(1)	7084(1)	10(1)
O(1)	1783(1)	5384(3)	1(3)	15(1)
O(2)	1590(1)	3410(3)	1573(3)	17(1)
O(3)	1627(1)	3013(3)	−884(3)	18(1)
O(4)	2461(1)	3550(3)	672(3)	22(1)
O(5)	4296(1)	2771(3)	6868(3)	15(1)
O(6)	4850(1)	4818(3)	6403(3)	17(1)
O(7)	3874(1)	4828(3)	5753(3)	18(1)
O(8)	4450(1)	3316(3)	4477(3)	18(1)
O(9)	1221(1)	7808(3)	−609(3)	21(1)
O(10)	1110(1)	8572(3)	−3086(3)	18(1)
O(11)	1072(1)	10313(3)	−1225(3)	21(1)
O(12)	346(1)	8591(3)	−1722(4)	24(1)
O(13)	2212(1)	6678(3)	2591(3)	20(1)
O(14)	2307(1)	6939(3)	5159(3)	18(1)
O(15)	2258(1)	4561(3)	4082(3)	19(1)
O(16)	3039(1)	6021(3)	3989(3)	21(1)
O(17)	3686(1)	7860(3)	6084(3)	14(1)
O(18)	4655(1)	7631(3)	6682(3)	15(1)
O(19)	4187(1)	9927(3)	7006(3)	16(1)
O(20)	4077(1)	7888(3)	8558(3)	16(1)
O(21)	5084(1)	1052(3)	5927(3)	22(1)
O(22)	1576(1)	9088(3)	2027(3)	23(1)
O(23)	673(2)	10638(7)	1258(5)	89(2)

[a] *U*(eq) is defined as one-third of the trace of the orthogonalized U_{ij} tensor. [b] The occupancies of Ti and Ga in M(3) are respectively 0.53(1) and 0.47(1). [c] The occupancies of Ti and Ga in M(4) are respectively 0.74(1) and 0.26(1).

Table 3. Atomic Coordinates ($\times 10^4$) and Thermal Parameters (Å^2 $\times$ 10^3) for **NGP-1**

	x	*y*	*z*	*U*(eq)[a]
Ga(1)	369(1)	−4298(1)	1433(1)	13(1)
M(2)[b]	94(1)	786(1)	772(1)	13(1)
M(3)[c]	−668(1)	−1954(1)	870(1)	12(1)
P(1)	0	−191(1)	2500	14(1)
P(2)	295(1)	−6647(1)	483(1)	13(1)
P(3)	−1157(1)	−4221(1)	1433(1)	14(1)
P(4)	1444(1)	163(1)	509(1)	15(1)
O(1)	−610(2)	−932(3)	1823(2)	18(1)
O(2)	302(2)	583(3)	2011(2)	19(1)
O(3)	655(2)	−5784(3)	1249(2)	18(1)
O(4)	377(2)	−3855(3)	327(2)	17(1)
O(5)	−831(2)	−2973(3)	−142(2)	16(1)
O(6)	72(2)	2378(3)	904(2)	19(1)
O(7)	−500(2)	−4757(3)	1402(3)	20(1)
O(8)	−1203(2)	−2959(3)	1270(3)	19(1)
O(9)	1126(2)	−4448(3)	2626(2)	18(1)
O(10)	−1839(2)	−4789(3)	702(2)	22(1)
O(11)	1127(2)	537(3)	1144(2)	19(1)
O(12)	−974(2)	757(3)	142(2)	18(1)
O(13)	−1526(2)	−1165(3)	24(2)	17(1)
O(14)	2208(2)	−320(3)	1105(3)	25(1)
O(15)	−10(2)	−925(3)	525(2)	13(1)
O(16)	252(2)	−2711(3)	1645(2)	16(1)

[a] *U*(eq) is defined as one-third of the trace of the orthogonalized U_{ij} tensor. [b] The occupancies of Ni and Ga in M(2) are respectively 0.14(1) and 0.86(1). [c] The occupancies of Ni and Ga in M(3) are respectively 0.10(1) and 0.90(1).

Magnetic Susceptibility, UV−Visible Spectrum, and EPR Measurements. Powder samples, 100 mg for each of **TGP-1** and **NGP-1**, were used to collect variable-temperature magnetic susceptibility [$\chi(T)$] data from 2 to 300 K in a magnetic field of 0.5 T using a Quantum Design SQUID magnetometer. The measured susceptibility data were corrected for core diamagnetism.[27] The UV−visible spectrum (UV−vis) was measured on a Hitachi U-3310 spectrophotometer. X-band electron paramagnetic resonance (EPR) spectra were recorded on a powder sample of **TGP-1** at 77 K with a Bruker EMX-10 spectrometer. The *g* values of these signals were measured relative to DPPH ($g = 2.0036$).

Table 4. Selected Bond Lengths (Å) for **TGP-1** and **Ti-free TGP-1**[a]

TGP-1		**Ti-free TGP-1**	
Ga(1)−O(7)	1.816(3)	Ga(1)−O(7)	1.820(2)
Ga(1)−O(16)	1.808(3)	Ga(1)−O(16)	1.804(2)
Ga(1)−O(17)	1.854(3)	Ga(1)−O(17)	1.848(2)
Ga(1)−O(20)#1	1.833(3)	Ga(1)−O(20)#1	1.835(2)
Ga−O_{ave}	1.828	Ga−O_{ave}	1.827
Ga(2)−O(2)	1.818(3)	Ga(2)−O(2)	1.816(2)
Ga(2)−O(3)#2	1.809(3)	Ga(2)−O(3)#3	1.817(2)
Ga(2)−O(11)#3	1.821(3)	Ga(2)−O(11)#2	1.816(2)
Ga(2)−O(15)	1.827(3)	Ga(2)−O(15)	1.830(2)
Ga−O_{ave}	1.819	Ga−O_{ave}	1.820
M(3)−O(5)	1.956(3)	Ga(3)−O(5)	1.928(2)
M(3)−O(6)#4	1.914(3)	Ga(3)−O(6)#4	1.898(2)
M(3)−O(8)#2	1.967(3)	Ga(3)−O(8)#3	1.917(2)
M(3)−O(18)#4	2.018(3)	Ga(3)−O(18)#4	1.995(2)
M(3)−O(19)#5	2.042(3)	Ga(3)−O(19)#5	2.004(2)
M(3)−O(21)	2.106(3)	Ga(3)−O(21)	2.085(2)
M−O_{ave}	2.001	Ga−O_{ave}	1.971
M(4)−O(1)	2.028(3)	Ga(4)−O(1)	1.956(2)
M(4)−O(9)	1.977(3)	Ga(4)−O(9)	1.925(2)
M(4)−O(10)#3	2.022(3)	Ga(4)−O(10)#2	1.965(2)
M(4)−O(13)	1.987(3)	Ga(4)−O(13)	1.934(2)
M(4)−O(14)#1	2.001(3)	Ga(4)−O(14)#1	1.960(2)
M(4)−O(22)	2.134(3)	Ga(4)−O(22)	2.078(2)
M−O_{ave}	2.025	Ga−O_{ave}	1.970

[a] Symmetry transformations used to generate equivalent atoms: (#1) x, $-y + 3/2$, $z - 1/2$; (#2) x, $-y + 3/2$, $z + 1/2$; (#3) x,$-y + 1/2$, $z + 1/2$; (#4) $-x + 1$, $y - 1/2$, $-z + 3/2$; (#5) x, $y - 1$, z.

Table 5. Selected Bond Lengths (Å) for **NGP-1**[a]

Ga(1)−O(7)	1.870(4)	P(1)−O(1)	1.531(4)
Ga(1)−O(9)	1.881(3)	P(1)−O(1)#2	1.531(4)
Ga(1)−O(4)	1.903(3)	P(1)−O(2)#2	1.538(4)
Ga(1)−O(3)	1.941(3)	P(1)−O(2)	1.538(4)
Ga(1)−O(16)	1.965(3)		
		P(2)−O(5)#3	1.530(4)
M(2)−O(2)	1.896(3)	P(2)−O(3)	1.533(3)
M(2)−O(6)	1.918(4)	P(2)−O(6)#4	1.534(4)
M(2)−O(11)	1.971(4)	P(2)−O(4)#3	1.544(4)
M(2)−O(12)	1.979(4)		
M(2)−O(15)#1	2.067(3)	P(3)−O(8)	1.529(4)
M(2)−O(15)	2.078(3)	P(3)−O(7)	1.534(4)
		P(3)−O(10)	1.536(4)
M(3)−O(13)	1.933(3)	P(3)−O(9)#2	1.543(4)
M(3)−O(8)	1.946(3)		
M(3)−O(1)	1.947(3)	P(4)−O(12)#1	1.535(4)
M(3)−O(5)	1.964(3)	P(4)−O(11)	1.537(4)
M(3)−O(16)	1.970(3)	P(4)−O(13)#1	1.539(4)
M(3)−O(15)	2.105(3)	P(4)−O(14)	1.548(4)

[a] Symmetry transformations used to generate equivalent atoms: (#1) $-x$, $-y$, $-z$; (#2) $-x$, y, $-z + 1/2$; (#3) $-x$, $-y - 1$, $-z$; (#4) x, $y - 1$, z; (#5) x, $y + 1$, z.

Results and Discussion

The unique structure of **TGP-1** consists of $M(H_2O)O_5$ octahedra and GaO_4 and PO_4 tetrahedra. As depicted in

(27) Selwood, P. W. *Magnetochemistry*; Interscience: New York, 1956.

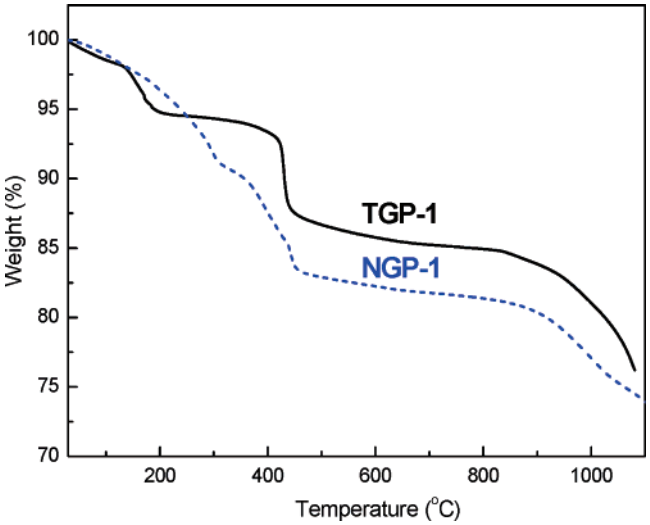

Figure 1. Thermogravimetric curves for **TGP-1** (solid line) and **NGP-1** (dash line) in flowing N_2 at 10 °C min^{-1}.

Figure 2, four independent metal sites are observed in the asymmetric unit: two gallium sites, Ga(1) and Ga(2), in four-coordination and two Ti/Ga mixed metal sites, M(3) and M(4), in six-coordination. The results from bond-valence-sum calculations, being 3.08, 3.14, 3.19, and 3.23 vu, respectively for the four metal sites, indicate all metals are trivalent. The incorporated titanium ions are thus Ti^{3+}, in contrast to the Ti^{4+} ions observed in most previously synthesized molecular sieves.[5,12] Another striking feature of **TGP-1** is that it possesses chunky layers (Figure 3) which are exceptionally thick, with a thickness of ~2.5 nm, coinciding with the *a*-axial length, and are highly porous. The layers are running along *a* with diprotonated piperazine and water molecules positioned between. There are two-dimensional intersecting channels within each layer: two arrays along *b* and two along *c*. All channel intersections are occupied by $(H_2PIP)^{2+}$ ions. In total, two-third of $(H_2PIP)^{2+}$ ions are residing in the intralayer space and one-third in the interlayer space. Adjacent layers are close with unusually narrow separation (<3 Å), where strong H bonds exist between the anionic layers and amine cations. Consequently, the architecture of **TGP-1**, with guest-ion density (2.47 organic cations/1000 $Å^3$) comparable to 3D MnGaPO-4[16] (2.45 molecules/1000 $Å^3$) but lower than typical 2D materials (>3.0 molecules/1000 $Å^3$)[28] and an estimated 32% solvent-accessible volume,[29] can be viewed as mimicing a porous 3D network.

This nanosized layer may be viewed as a composite of four octahedra−tetrahedra sheets stacking in ABB^iA^i sequence (^{i} denotes inversion) with pendent PO_4 tetrahedra flanking the layers. As shown in Figure 4, the porous sheet built up with $M_2(H_2O)(PO_4)_2$ single four-rings (S4Rs) is a 4.8^2 net.[30] It is also isotypic with the chiral layers in [(1*S*,2*S*)-H_2DACH][Ga_2(1*S*,2*S*-DACH)$(HPO_4)(PO_4)_2$].[31] Sheets A and B, being connected through tetrahedra of Ga(1)O_4 and P(4)O_4, form 2D intersecting channels that contain $4^26^28^210^2$ cages, as shown in Figure 5. Another type of cage, $4^26^28^2$, is also observed in the two inversion-related sheets B and B^i, which, via M(3)O_6 and P(2)O_4, are fused into a condensed doublet positioned in the central part of the thick layer. Sheets A and B have the same connectivity but differ in Ti concentration due to different octahedral centers (M(4)in A and M(3) in B). 75% of the M(4) centers are titanium, whereas only half of the M(3) centers contain titanium. The degree of Ti incorporation is therefore higher in the shallow sheets A than in the central sheets B.

An X-band EPR spectrum (Figure 6) recorded at 77 K on a powder sample revealed a sharp peak in the vicinity of $g_{iso} = 1.9$, a value comparable with that reported on Ti^{3+}-doped material.[32] The UV−vis spectrum of **TGP-1** has a broad band centered at ~270 nm, unlike tetrahedrally (~205 nm) and octahedrally (~225 nm) Ti^{4+}-substituted structures.[33] With one unpaired electron, the Ti^{3+} ion is a Kramers ion, with the ground state in an octahedral field, being $^2T_2$, and has an air-sensitive nature that has been an obstacle to explorations of its magnetic behavior.[34] However, the Ti^{3+} ion trapped in the extended framework of TGP-1 seemed stablized enough for magnetic study. According to the temperature-dependence molar magnetic susceptibility data shown in Figure 7, **TGP-1** showed an observed magnetic moment lower than its spin-only value, due to spin−orbit coupling, and did not seem to follow the Curie−Weiss law well, since its χ_{MT} values dropped mildly as the temperatures decreased. Its antiferromagnetic behavior was observed to reach a minimum at 10 K with a constant χ_{MT} value of 0.37 cm^3 K mol^{-1}, and then it conversely increased a bit under 6 K, indicating a possible ferromagnetic interaction between Ti^{3+} ions. Considering the nearest distances, M(4)···M(4)

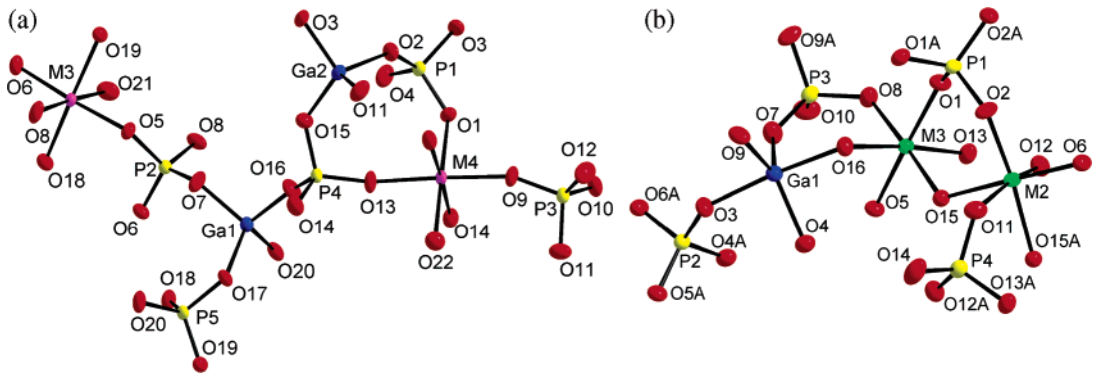

Figure 2. ORTEP drawings showing the labeling scheme and local coordination of the asymmetric unit in (a) **TGP-1** and (b) **NGP-1**. The hydrogen atoms of water and hydroxyl groups are not shown. Thermal ellipsoids are drawn with 50% probability.

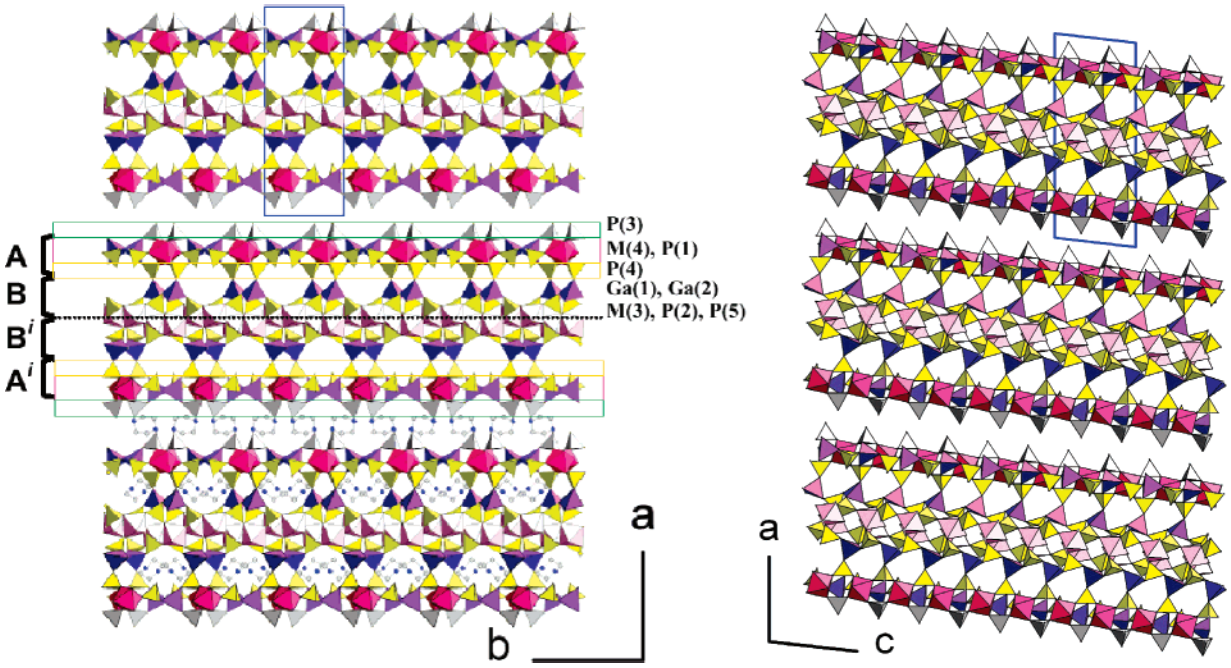

Figure 3. Perspective views of the structure of **TGP-1**. (Left) projection along the *c*-axis; (right) projection along the *b*-axis. The layer is comprised of four polyhedral sheets stacking in ABB^iA^i sequence. Intersecting channels are observed in both directions. The concentration of Ti^{3+} ions is higher in the shallow sheets A than the deeper sheets B. Various polyhdera: GaO_4, purple; $M(3)O_5(H_2O)$, pink; $M(4)O_5(H_2O)$, red; intralayer PO_4, yellow; and pendent PO_4, gray. For clarity, $(H_2PIP)^{2+}$ ions are omitted from the first two layers and the right figure.

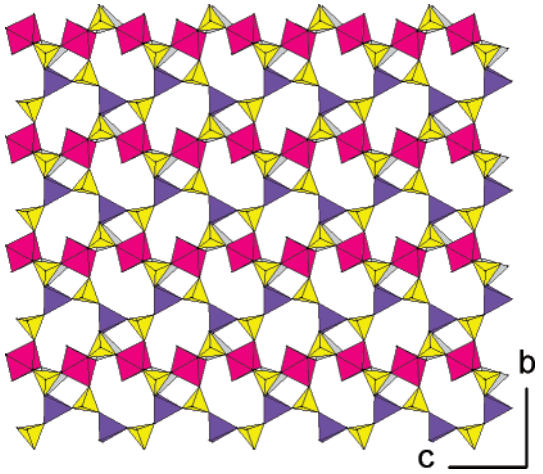

Figure 4. Section of sheet A plus pendent PO_4 groups (gray tetrahedra underneath) showing the S4Rs and 8R windows. Sheet B is similar to A except the Ti concentration in M centers.

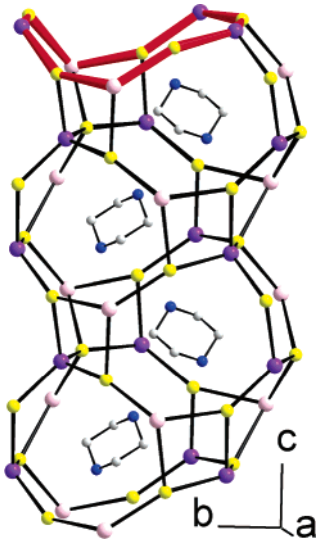

Figure 5. $4^26^28^210^2$ cage in **TGP-1** showing the 10-ring window (in red lines) toward [001].

4.954 Å within sheets A, M(3)···M(3) 5.133 Å within sheets B, and M(3)···M(4) 9.126 Å between neighboring sheets A and B, exchange couplings between the Ti^{3+} centers should be confined within individual sheets A or B. It is noticed that the pink color of **TGP-1** crystals will fade upon heating or exposing to air for weeks. Oxidations of the paramagnetic Ti^{3+} to diamagnetic Ti^{4+} centers should likely occur. This may also partially account for the effective magnetic moment (μ_{eff}) of 1.41 μ_B, determined from the equation $\mu_{eff} = 2.828(\chi_M T)^{1/2}$ at 300 K, being lower than the expected value of 1.73 μ_B of an isolated d^1 system.

To prepare the corresponding Ti-free GaPO compound, we have tried to eliminate titanium from the reactants. However, it always resulted in unknown phases. Meanwhile, a tiny amount of colorless crystals that always grew together with the pink ones was discovered from reactions carried out under nonoptimal conditions for **TGP-1**. EPMA data of the colorless crystals showed no titanium content at all. The colorless crystal was analyzed to be isostructural with **TGP-1**

(28) The value was estimated from layered materials encapsulating organic molecules of similar size to piperazine.
(29) Spek, L. *Acta Crystallogr. Sect. A* **1990**, *46*, C34.
(30) Wells, A. F. *Further Studies of Three-Dimensional Nets*; American Crystallographic Association: Buffalo, NY, 1979.
(31) Lin, C. H.; Wang, S. L. *Inorg. Chem.* **2001**, *40*, 2918.
(32) Rojo, J. M.; Mesa, J. L.; Calvo, R.; Lezama, L. Rojo, T. *J. Mater. Chem.* **1998**, *8*, 1423−1426.
(33) Blasco, T.; Camblor, M. A.; Corma A.; Pérez-Pariente J. *J. Am. Chem. Soc.* **1993**, *115*, 11806.
(34) Carlin, R. L. In *Magnetochemistry*; Springer: Berlin, 1996; pp 58 and 154.

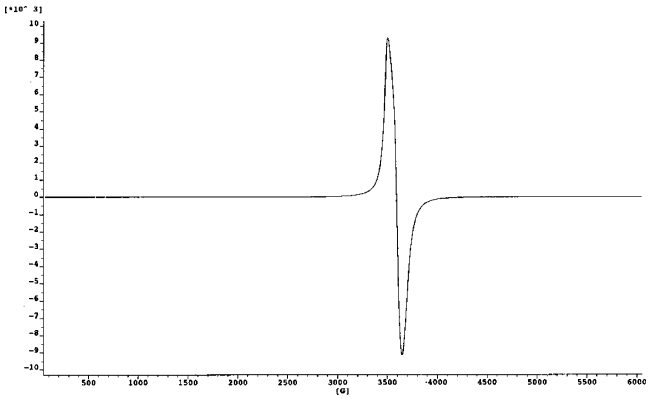

Figure 6. X-band EPR spectrum of **TGP-1** at 77 K.

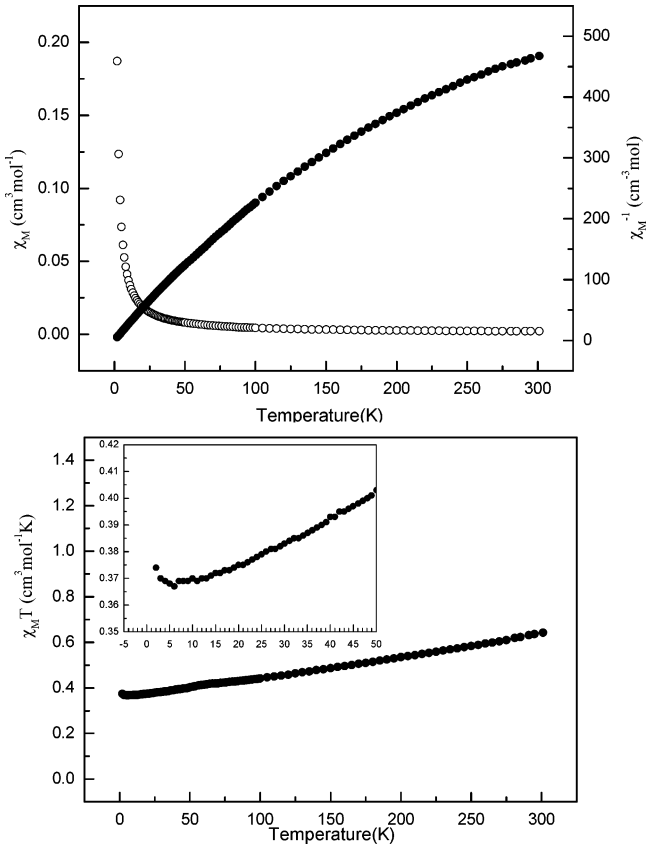

Figure 7. Temperature-dependent magnetic susceptibility data for **TGP-1**: (Top) χ_M vs T (○) and χ_M^{-1} vs T (●) plots; (Bottom) χ_{MT} vs T plot, showing a declined curve with antiferromagnetic behavior but ferromagnetic tendency at termperatures lower than 6 K (see the inset).

and has the composition of $[H_2PIP]_3[Ga_8(H_2O)_4(PO_4)_{10}]\cdot 2H_2O$, namely designated as **Ti-free TGP-1**.[35] Averaged bond distances (Å) in the **Ti-free TGP-1** are Ga(1)−O, 1.827; Ga(2)−O, 1.820; Ga(3)−O, 1.971; Ga(4)−O, 1.970. In comparison between the two structures, the following is observed from **Ti-free TGP-1** to **TGP-1**: (i) the Ga−O bond distances in GaO_6 octahedra [M(3)−O vs Ga(3)−O and M(4)-O vs Ga(4)−O] are lengthened by 0.03−0.06 Å, and (ii) the cell volume is increased by 27 Å^3. According to Shannon,[36] the effective crystal radii for six-coordinated Ga^{3+}, Ti^{3+}, and Ti^{4+} ions are respectively 0.76, 0.81, and

(35) See Supporting Information for detailed crystal data.
(36) Shannon, R. D. *Acta Crystallogr. Sect. A* **1976**, *32*, 751.

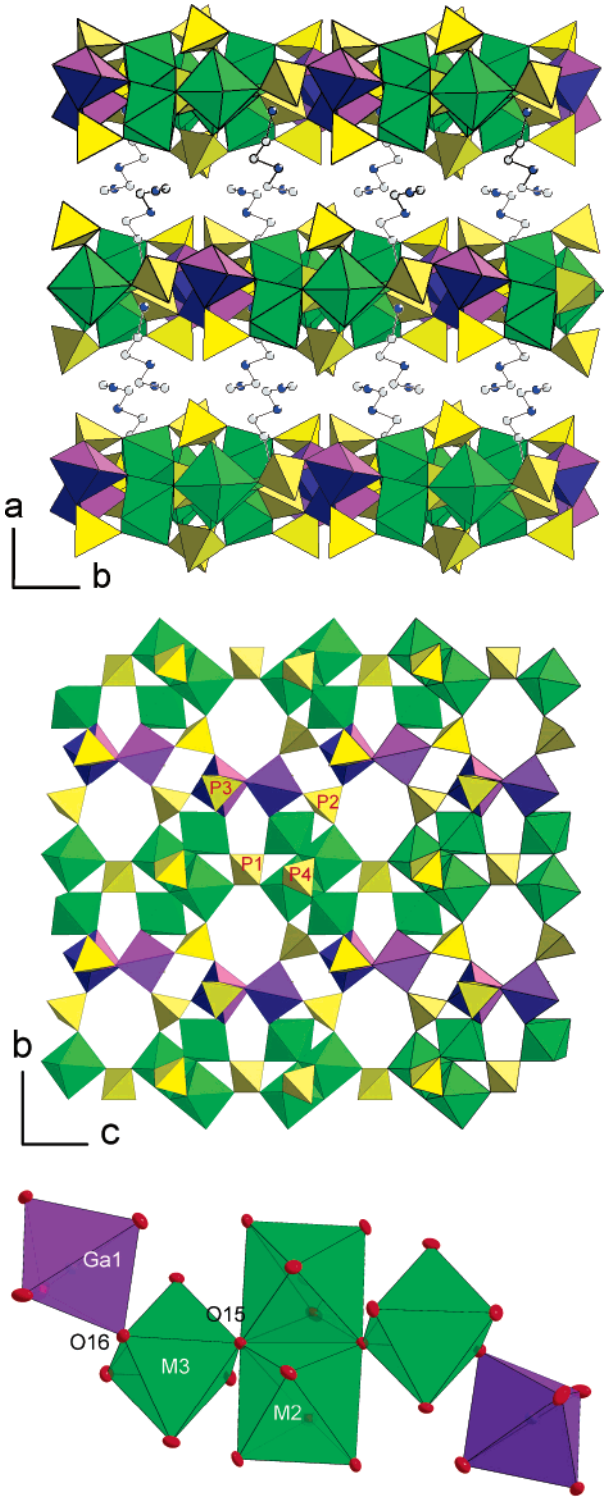

Figure 8. Structure of **NGP-1**. (Top) Projection *c* showing the elevation of layers and organic cations. (Middle) Section of an anionic layer. (Bottom) The hexameric $M_6(OH)_4O_{24}$ cluster unit. Polyhedral representation for GaO_5 in purple and $M(OH)_2O_4$ in green.

0.745 Å. The observed expansion in bond distance and cell volume further confirms that the valency of titanium in **TGP-1** is 3+.

The structure of **NGP-1** is also two-dimensional (Figure 8) and the layers are built up with $Ga(OH)O_4$ trigonal bipyramids, $M(OH)_2O_4$ octahedra, and PO_4 and HPO_4 tetrahedra. The asymmetric unit (Figure 2) contains three

independent metal sites: one five-coordinated site, Ga(1), which is solely occupied by Ga^{3+} ions, and two six-coordinated sites, M(2) and M(3) sites, which are mixed with Ni^{2+} and Ga^{3+} ions. These three kinds of polyhedra are connected via bridging OH groups: Ga(1)[5by] and M(3)[6o] share a common vertex of O(16)H, and M(2)[6o] and M(3)[6o] share a common vertex of O(15)H. In the M(2) octahedron, the edge linked by two O(15)H groups falls on a center of inversion. Hence, a hexameric unit, $M_6(OH)_4O_{24}$, shown in Figure 7, is generated with an edge-sharing bioctahedra with two M(2)[6o] residing in the center. Bond-valence sums calculated for μ_3-O(15) and μ_2-O(16) are respectively 1.1 and 1.0 vu, which indicate typical values for hydroxy oxygens. It is noted that, excluding two trigonal bipyramids, the central tetranuclear cluster resembles that of the iron clusters in the chain structure of $(H_2PIP)_{1.5}[Fe_2(OH)(H_2PO_4)(HPO_4)_2(PO_4)]\cdot 0.5H_2O$.[37]

The inorganic layer of **NGP-1** can be described as constructed from non-close-packed $M_6(OH)_4O_{24}$ clusters that are interconnected by P(1)O_4 along *c* and P(2)O_4 along *b* into a layer (Figure 7). Hydrogen phosphate groups are pendent to layer where the HP(3)O_4 tetrahedra connect with two neighboring hexamers along *c* and HP(4)O_4 to one hexamer only. Between the layers are protonated DETA and water molecules. The amount of incorporated Ni^{2+} ions, which was initially determined from structure refinement, are 0.15Ni and 0.85Ga on the M(2) site and 0.10Ni and 0.90Ga on the M(3) site. Accordingly, more than half of the DETA molecules are necessarily triprotonated to balance the charge. A magnetic susceptibility study on a bulk sample of **NGP-1** showed that it followed Curie−Weiss law with Weiss constant $\theta = -4.8$ K, Curie constant $C = 0.197$, and the effective magnetic moment $\mu_{eff} = 2.51\ \mu_B$, which is lower than the spin-only value of 2.83 μ_B for a d^8 system. The observed value merely corresponds to 0.39 mol of Ni^{2+} ions per formula unit. The results from EPMA and ICP-AES measurements revealed that the Ni/Ga ratios were separately 0.13:5.87 and 0.32:5.68, indicating that the NGP-1 phase is likely a solid solution. The extent of protonation for the DETA molecules therefore varies with the content of Ni^{2+} ions in **NGP-1**. So far, the maximum ratio of Ni/Ga has been determined from single-crystal analysis to be 0.5:5.5.

In contrast to **Ti-free TGP-1**, the **Ni-free NGP-1** can be obtained directly from the same reaction mixture for preparing **NGP-1** just by eliminating the transition metals. The colorless crystals of **Ni-free NGP-1**, with the formula of $[H_3(C_4H_{13}N_3)_2][Ga_6(OH)_4(PO_4)_3(HPO_4)_4]\cdot 2H_2O$,[35] retain exactly the same layer structure as the green crystals of **NGP-1** but a slightly lower protonation. To date, only five organically templated 2D GaPO materials[31,38−42] have been reported, and their Ga/P ratios range as 1:1, 6:7, 2:3, and 1:2 (Table 6). It is noted that **Ni-free NGP-1** and the recently reported **JGP-L1**,[40] $(C_8H_{28}N_5)[Ga_6(OH)_4(PO_4)_5(HPO_4)_2]\cdot 3H_2O$, are polytypes.[43] The later crystallizes in the space group $Pna2_1$ instead of *C*2/*c*, with nominally high crystal symmetry but no inversion in hexameric clusters. In addition, **Ni-free NGP-1** has a higher HPO_4 to PO_4 ratio (4:3 vs 2:5) and hence less negatively charged inorganic layers (−3 vs −5).

Table 6. Summary of Atomic Ratios, Cations, and Inorganic Compositions for Organically Templated Gallophosphates with Layer Structures

	Ga/P	cation	amine name	layer composition	ref
1	1:1	$[C_2H_{10}N_2]^{2+}$	ethylenediamine	$[Ga(OH)(PO_4)]$	38
2	1:1	none	4,4′-bipyridine	$[Ga_2(4,4\text{-bpy})(PO_4)_2]$	39
3	6:7	$[C_8H_{23}N_5]^{5+}$	tetraethylene-pentamine	$[Ga_6(OH)_4(HPO_4)_2(PO_4)_5]$	40
4	6:7	$[C_4H_{16}N_3]^{3+}$	diethylene-triamine	$[Ga_6(OH)_4(HPO_4)_4(PO_4)_3]$	this work[a]
5	4:5	$[C_4H_{12}N_2]^{2+}$	piperazine	$[Ga_4(H_2O)_2(PO_4)_5]$	this work[b]
6	2:3	$[C_6H_{16}N_2]^{2+}$	1,2-diamino-cyclohexane	$[Ga_2(C_6H_{16}N_2)(HPO_4)(PO_4)_2]$	31
7	1:2	none	2,2′-bipyridine	$[Ga(2,2\text{-bpy})(HPO_4)(H_2PO_4)]$	41
8	1:2	$[C_5H_6N]^+$	pyridine	$[Ga(H_2O)_2(HPO_4)_2]]$	42
9	1:2	$[C_3H_5N_2]^+$	imidazole	$[Ga(H_2O)_2(HPO_4)_2]$	42

[a] **Ni-free NGP-1**. [b] **Ti-free TGP-1**.

In conclusion, the first unique titanium- and nickel-incorporated gallophosphates, **TGP-1** and **NGP-1**, together with nonincorporated forms have been successfully prepared and their structures are clearly elucidated. **TGP-1** has nanosized layers wherein intersecting channels and cages are residing, and the distribution of titanium diminishes along the depth of the layer. In comparison with most previously synthesized molecular sieves that have Ti atoms in the oxidation state of +4, **TGP-1** provides the first example where paramagnetic Ti^{3+} centers can be synthesized as an integral part of the microporous framework. **TGP-1** and **NGP-1** added two new structure types to the MGaPO system. Despite most reported MGaPOs, where TM ions occupy tetrahedral sites, this study shows an opposite trend where both titanium and nickel prefer six-coordinated to four- or five-coordinated sites. Besides, these two novel structures contain only mixed sites, unlike our earlier unique MGaPOs, which have independent TM sites.[14,16−18] Will independent Ti^{3+} or Ni^{2+} sites appear in new MGaPO structures? Further research on this trend is in progress.

Acknowledgment. We are grateful to the National Science Council of the Republic of China for support of this work (NSC 92-2113-M-007-029).

Supporting Information Available: Crystallographic data (CIF) for **TGP-1**, **Ti-free TGP-1**, **NGP-1**, and **Ni-free NGP-1**; plot of hydrogen bonds in **TGP-1**; magnetic susceptibility data and fitting curves for **NGP-1**; and UV−vis spectrum for **TGP-1**. This material is available free of charge via the Internet at http://pubs.acs.org.

IC0494556

(37) Zima, V.; Lii K. H. *J. Chem. Soc., Dalton Trans.* **1998**, 4109.
(38) Jones, R. H.; Thomas, J. M.; Huo, Q.; Xu, R.; Hursthouse, M. B.; Chen, J. *J. Chem. Soc., Chem. Commun.* **1991**, 1520.
(39) Chen, C. Y.; Lii, K. H.; Jacobson, A. J. *J. Solid State Chem.* **2003**, *172*, 252.
(40) Yang, Y.; Liu, Y.; Mu, Z.; Ye, L.; Hu, T.; Chen, C.; Pang, W. *J. Solid State Chem.* **2004**, *177*, 696
(41) Lin, Z. E.; Zhang, J.; Sun, Y. Q.; Yang, G. Y. *Inorg. Chem.* **2003**, *43*, 797.
(42) Leech, M. A.; Cowley, A. R.; Prout, K.; Chippindale, A. M. *Chem. Mater.* **1998**, *10*, 451.
(43) Müller, U. *Inorganic Structural Chemistry*; John Wiley & Sons: New York, 1992.